Optics and Laser Technology 127 (2020) 106192

Contents lists available at ScienceDirect

Optics and Laser Technology

journal homepage: www.elsevier.com/locate/optlastec

Enhanced short temporal coherence length measurement using Newton's rings interference

W.A. Ramadan[a], H.H. Wahba[a,b], A.S. El-Tawargy[a,*]

[a] Physics Department, Faculty of Science, Damietta University, 34517 New Damietta City, Egypt
[b] Physics Department, Faculty of Science, Taif University, Taif, Al-Haweiah, 21974, Saudi Arabia

HIGHLIGHTS

- Newton's rings to measure temporal coherence lengths of light emitting diodes.
- This method is based on accurate visibility determination of Newton's rings.
- The tolerance of the temporal coherence length measurement is less than 5%.
- We expect applying this method on pulsed lasers.

ARTICLE INFO

Keywords:
Light emitting diode (LED)
Newton's rings
Temporal coherence length (TCL)

ABSTRACT

In this work, we used a simple accurate method to measure the short temporal coherence length of a light emitting diode. This method is based on accurate visibility determination of Newton's ring fringes. The visibility of Newton's rings has its maximum value around the position of contact point between the spherical and the plane surfaces while it decreases, until vanishing, with moving towards the outer rings. This is due to the gradually increasing thickness of the air gap separating the two surfaces; starting from zero at the contact point. When the lowest detectable value of visibility tends to zero, there are only two interfered rays which are temporarily separated by the value of the temporal coherence length of the used light source. By detecting these two rays and calculating their optical paths, it was easy to evaluate the temporal coherence length of the used light source. For the purpose of accuracy enhancement, both intensity and visibility calculations of each detected interference order were automatically determined by employing an algorithm prepared using MATLAB software environment. Moreover, tracing the real optical paths of the two interfered rays forming the interference enabled us to calculate the spatial distance which is separating them without any approximation. This distance was too short ($<$ 20 nm) which means that we almost dealt with a pure temporal coherency. In this work, three commercial light emitting diode sources with different wavelengths were investigated and their temporal coherence length values were determined. Investigation of tolerance of temporal coherence length measurement was discussed.

1. Introduction

A light source can be characterized by two types of optical coherency; spatial and temporal. The former measures the phase correlation between two points locate transversely to the direction of propagation while the latter measures the phase correlation between two points locate along the direction of propagation [1–3]. Therefore, the spatial coherence reflects the uniformity of the phase of the wavefront while temporal coherence describes the longevity of the phase as a function of time. Moreover, spatial coherence gives the ability of shaping the emitted beam, for instance by using a spatial light modulator [4], and it is extremely important for the light penetration depth through the living tissues in the therapeutic purposes [4–7]. Deng et al. concluded that the sharpness of an image is linearly proportional to the spatial coherence of the illuminating source while the speckle contrast is linearly proportional to the source's temporal coherency [8]. Both uniformity and sharpness of an image can be optimized by selecting suitable levels of both types of coherency of the used light source [8]. Furthermore, coherence time (τ) is the maximum delay time between two successive waves which still able to produce interference. It can be

* Corresponding author.
E-mail address: a_tawargy@du.edu.eg (A.S. El-Tawargy).

https://doi.org/10.1016/j.optlastec.2020.106192
Received 30 January 2020; Received in revised form 24 February 2020; Accepted 28 February 2020

defined as the ratio between the temporal coherence length (TCL) and the speed of light [1]. Therefore, TCL expresses the largest difference between optical pathlengths of two rays before they can no longer interfere.

Lasers have high degree of both spatial and temporal coherency so that they are used to produce sharp images in holographic displays and 3D imaging [8]. However, significant speckles are always accompanied with lasers because of the long coherence lengths which affecting the quality of images [9–13]. To suppress this speckle, there are several techniques such as applying phase gratings or diffusers. However, these solutions increase both complexity and costs of the optical system and might decrease the bandwidth of the image [8]. Alternatively, using a partially coherent light source such as a light emitting diode (LED) or an organic light emitting diode (OLED) is a good candidate to reduce speckle because of their low temporal coherency [8,14–16]. LEDs are promising competitors for many applications in the daily use; e.g. lighting, displays, visible light communications, biomedical instruments and photonic devices [4,17–22]. However, an additional spatial filter would be required, in some applications, to select a certain spot of light from the LED in order to increase the spatial coherence to some extent and hence increase the sharpness of the image [8]. In general, studying both spatial and temporal coherence properties of LEDs and OLEDs got more attentions in the recent years with more focusing on the former one [1,2,4,6,8,15,16,23–29].

Optical interferometry is an interesting tool offering solutions to characterize synthesized waveguides such as those planar passive waveguides prepared by ion-exchange method [30] and by UV-laser lithographic method [31]. The problem of measuring refractive indices of highly refractive index liquids was overcome using an interferometric method called "lens-fibre interference" [32]. Moreover, optical interferometry can detect tiny changes of refractive index profiles of fibrous materials experienced mechanical stresses [33–38]. Due to their accuracy and feasibility, optical interferometric based techniques are applicable in coherency measurements. For instance, Duarte et al. and Saxena et al. investigated, interferometrically, the spatial coherence of OLEDs using Young's double-slit experiment and inserting another single slit between the double slit and the used OLED [14,23]. They obtained clear fringes but they, actually, measured the coherency of the spatially filtered OLED not the spatial coherency of the OLED itself. Xie et al. used a telescope and a Young's double slit to measure the intrinsic spatial coherence length of OLEDs by the aid of a Fourier transform imaging system [4]. Due to the low visibility of their fringes, they integrated diffractive optical elements (DOEs) to improve it. Leppänen et al. measured the degree of temporal coherency and its associated coherence time of a LED by observing Stokes-parameter modulations of Michelson Interferometer [28]. On the other hand, Newton's rings interference is quite suitable for measuring coherence properties of light sources having short coherence lengths like LEDs [29]. Newton's fringes represent a distribution of alternate bright and dark concentric rings formed when a curved surface is placed on a flat surface. These two optical surfaces are usually having low values of reflectivity and arresting a thin film of air with a graded thickness [39,40]. The central ring is formed at the point of contact of the two optical surfaces and it is the most important advantage of Newton's interferometer where the optical path difference between the two interfered rays at the contact point is almost zero [41]. This ensures that one can count the fringes' order beginning from zero. This advantage is difficult to be found in another interferometer even with Fizeau fringes [42]. Recently, our group presented a theory to estimate the intensity distribution evolved from Newton's rings apparatus [41,43]. The distribution of Newton's rings basically depends on the geometrical parameters of the used curved surface as well as the temporal coherence length of the used light source. Therefore, for a certain curved surface, we can study the coherency of the illuminating source independently as will be explained below.

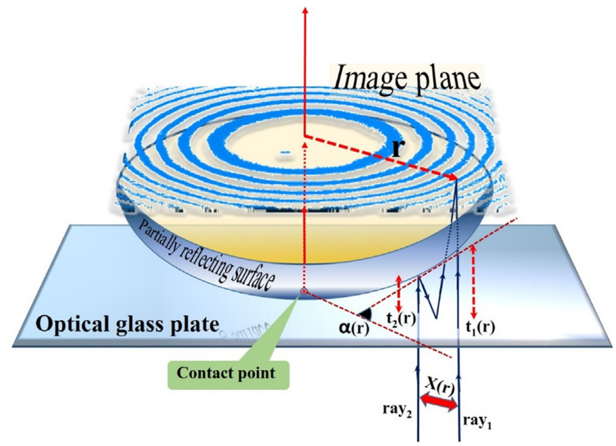

Fig. 1. The optical components used to produce Newton's ring fringes in transmission. r is the distance between the central point and any other point in the interference pattern. $X(r)$ is the spatial distance between the two interfered rays.

2. Theoretical considerations

When a curved surface is placed on a flat surface, a thin film of air having a graded thickness is arrested. If a collimated bundle of light rays falls on this optical setup as shown in Fig. 1, Newton's rings would be formed in transmission as a distribution of alternate bright and dark concentric rings. The central ring is formed in the middle at the position of the contact point between the curved surface and the flat surface. Moving away from the central ring towards the outer rings, the air gap between the two surfaces increases and the difference between geometrical pathlengths of the two interfered rays increases as well. Consequently, the interferometric visibility decreases until vanishing. The visibility V_n for any interference order n can be given by Eq. (1) [29,44].

$$V_n = \frac{I_{n,max} - I_{n,min}}{I_{n,max} + I_{n,min}}, \tag{1}$$

where, $I_{n,\text{min}}$ is the minimum of the intensities of two dark fringes enclosing the n^{th} bright fringe which having a maximum intensity $I_{n,\text{max}}$.

The last detectable fringe (before losing visibility) must be formed by an interference of only two rays [41]. This is an assurance that the TCL is the maximum length which is able to produce a detectable interference between two rays separated by a spatial distance $X(r)$, see Fig. 1. The optical setup has to be designed to produce an interference pattern contains the fringes, beginning from the central fringe until visibility vanishing, in a single shot. We can obtain this feature in a single shot by selecting the appropriate curved surface and optimizing the magnification of the imaging system. These conditions would be difficult to be verified for a light source characterized by a long coherence length and that is why the presented method is convenient for short coherent optical sources.

3. Experimental work

We used the optical setup shown in Fig. 2 in order to produce Newton's ring fringes in case of transmission. Three LEDs with different wavelengths (490 nm, 590 nm and 645 nm) were used as illuminating sources and in order to obtain their TCL values. The collimating lens was used to obtain a collimated bundle of rays from each LED. This bundle was permitted to fall on the optical system constituting the partially reflecting curved surface of radius of curvature 9.40 cm [43] which placed on the flat glass surface. The produced interference was imaged with a suitable magnification; 1.17 μm/pixel. The interference patterns were recorded by the attached CCD camera and digitally saved for the forthcoming analyses. Neither spatial filtering nor additional

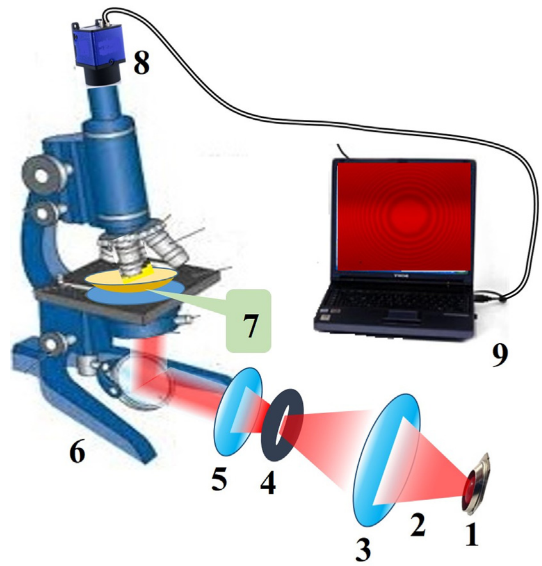

Fig. 2. The setup used for producing and capturing Newton's rings in transmission where (1) a LED, (2) a divergent beam, (3) a condensing lens, (4) an Iris diaphragm, (5) a collimating lens, (6) an optical microscope, (7) Newton's rings interference apparatus, (8) a CCD camera and (9) a computer for saving and analyzing the interferograms.

optical components were required to record suitable interference patterns. Additionally, each interference pattern was recorded as a single shot contains all the required information and no mechanical scanning was needed to capture the interference pattern.

4. Results and discussion

Fig. 3 shows the experimentally obtained raw interference patterns of Newton's rings using the optical setup shown in Fig. 2 with LEDs of different wavelengths; (a) 490 nm, (b) 590 nm and (c) 645 nm. As a first glance, these interferograms are almost free of noise since the speckle accompanied due to using LEDs is low. Moreover, one can notice that each image is characterized by a highly visible central ring fringe while the visibility decreases as the ring radius increases until vanishing before the image boards. Therefore, the interference patterns can be analyzed by extracting their intensity distributions. In contrast with Young's equidistant fringes [15], Fourier transformation can't be applied on the non-equidistant Newton's fringes to extract their phase distribution. However, it was sufficient to read the intensity distributions of the obtained patterns in our study. The intensity distribution of each interferogram was automatically read in one direction assuming that we have a radially symmetric curved surface, see Fig. 4. In addition, intensities of every ten adjacent pixels were averaged in order to reduce the, if exist, noises to their lowest limit. The automatically recorded intensity values were feed to a prepared MATLAB algorithm to determine the visibility (V_n) values, for the three different used LEDs, according to Eq. (1) and were plotted as shown in Fig. 5.

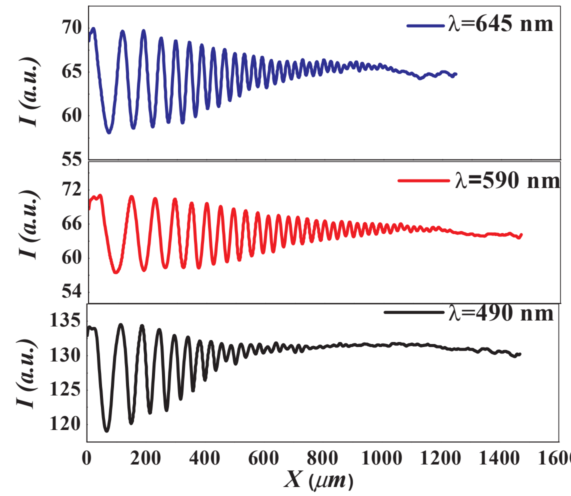

Fig. 4. The intensity distributions of the interference patterns shown in Fig. 3 where X starts from the central ring moving towards the most outer ring.

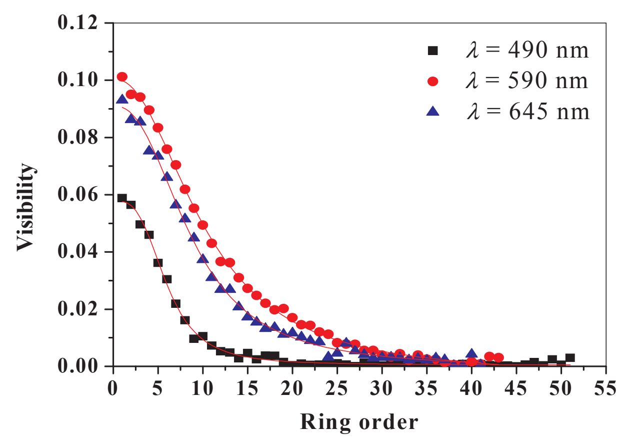

Fig. 5. The dotted points represent the visibility values as functions of the rings' order calculated for the interference patterns shown in Fig. 3. Solid curves represent the fittings, by the logistic function, of the drawn points.

As expected, Fig. 5 shows that a visibility curve has a maximum value at the position of the central fringe and it decays with increasing the fringes' order. In order to increase the accuracy of our procedure, we fitted the visibility data with a standard function which enabled detecting the minimum visibility value automatically. That is more efficient than the previous works [29,39] where they were counting the distinguishable minima of the intensity distribution curve. We found that each plotted curve in Fig. 5 obeys, and can be fitted by, the logistic function [45,46] which is described by the following equation.

$$V_n(n) = A_2 + \frac{A_1 - A_2}{1 + \left(\frac{n}{n_o}\right)^p}, \tag{2}$$

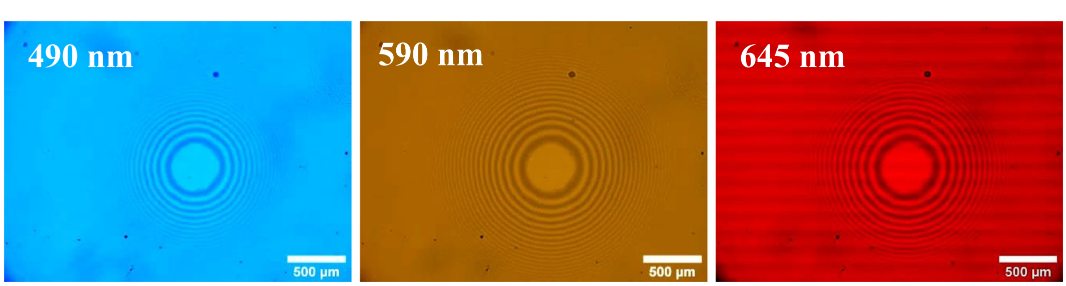

Fig. 3. The experimentally obtained interference patterns of Newton's rings, formed in transmission, with LEDs of different wavelengths.

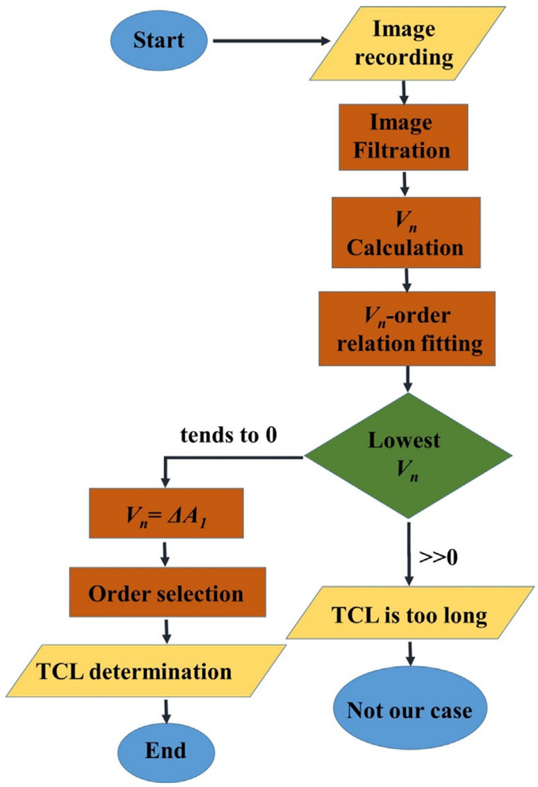

Fig. 6. Flowchart of the followed procedure to calculate the TCL of a LED.

where n represents the ring's order while V_n represents its corresponding visibility value. A_1 is the minimum value of the visibility while A_2 is its maximum value. n_o is the order at which the visibility reaches half of its maximum value. p is a constant controls the tendency of the fitting curve.

For higher orders of interference, the interferometric visibility drops to zero, i.e. A_2 approaches zero. In this case, Eq. (2) can be rewritten as follows;

$$V_n(n) = \frac{A_1}{1 + \left(\frac{n}{n_o}\right)^p}, \tag{3}$$

which by rearranging gives the following equation;

$$n(V_n) = n_o\left(\frac{A_1}{V_n} - 1\right)^{\frac{1}{p}}, \tag{4}$$

Fig. 6 shows the flowchart which summarizes our procedure from recording the interference pattern until calculating the visibility and calculating the TCL of a LED.

Practically, TCL is defined as the optical path difference when the interferometric visibility drops to zero [44]. Therefore, it can be definitely given as the product of the wavelength and the value of n corresponds to the minimum value of V_n.

$$TCL = \lambda n(Vn) \quad when \quad V_n \to 0, \tag{5}$$

Referring to Eq. (4), It is obvious that determination of the order n depends on three variables; n_o, A_1 and p. To evaluate the error propagation Δn in determining the order n, we had to consider the error evolved from each variable independently. Therefore, we applied the following relation;

$$\Delta n = \sqrt{\left(\frac{\partial n}{\partial n_o}\right)^2(\Delta n_o)^2 + \left(\frac{\partial n}{\partial A_1}\right)^2(\Delta A_1)^2 + \left(\frac{\partial n}{\partial p}\right)^2(\Delta p)^2}, \tag{6}$$

where,

Table 1
The values of the variables mentioned in Eqs. (4) and (6) and their corresponding standard deviation values for the three used LEDs. The calculated values of both TCL and τ are illustrated in the last two rows for the three LEDs.

λ (μm)	0.490	0.590	0.645
A_1	0.058	0.099	0.090
ΔA_1	0.79×10^{-3}	1.01×10^{-3}	1.01×10^{-3}
n_o	5.909	10.038	8.720
Δn_o	0.096	0.143	0.138
p	3.060	2.479	2.511
Δp	0.096	0.053	0.060
V_n	0.79×10^{-3}	1.01×10^{-3}	1.04×10^{-3}
$n(V_n)$	24	64	51
Δn	1.126	2.679	2.330
TCL (μm)	11.23–12.33	35.87–39.02	31.63–34.63
τ (fs)	37.4–41.1	119.6–130.1	105.5–115.4

$$\frac{\partial n}{\partial n_o} = \left(\frac{A_1}{Vn} - 1\right)^{\frac{1}{p}}, \tag{7}$$

$$\frac{\partial n}{\partial A_1} = \frac{n_o}{pVn}\left(\frac{A_1}{Vn} - 1\right)^{\frac{1}{p}-1}, \tag{8}$$

$$\frac{\partial n}{\partial p} = -\frac{n_o}{p^2}\left(\frac{A_1}{Vn} - 1\right)^{\frac{1}{p}}\ln\left(\frac{A_1}{Vn} - 1\right), \tag{9}$$

while Δn_o, ΔA_1 and Δp are the standard deviations of the parameters n_o, A_1 and p, respectively. By applying these calculations in the obtained visibility curves and performing fittings, we obtained the values illustrated in Table 1. However, for the reasons of singularity in Eq. (9), we considered $V_n = \Delta A_1$ instead of V_n equals absolute zero in our calculations. This approach is still acceptable where ΔA_1 is less than 1.01×10^{-3}. Based on the values of Δn, we calculated TCL values of the used LEDs which were varying between *ca.* 11 μm and *ca.* 39 μm as illustrated in Table 1. The corresponding temporal coherence time (τ) values were varying between *ca.* 37 fs and *ca.* 130 fs.

In addition to the error calculations of our measurements, we investigated the probability of spatial coherence contribution. Therefore, we estimated the distance $X(r)$ separating the two interfered rays as a function of the distance between the contact point and each point in the interferogram as illustrated in Fig. 1. $X(r)$ is given by the following equation [41];

$$X(r) = (t_1 + t_2)\tan(2\alpha(r)) \tag{10}$$

where, t_1 and t_2 are the air gap thicknesses for the first and the second interfered rays, respectively. $\alpha(r)$ is the angle of the curved surface's tangent at any point in the interference pattern, see Fig. 1. This distance was extracted by the same way used to estimate Newton's fringes in transmission, previously presented in reference [41]. Fig. 7 gives the calculated $X(r)$ values which varies from (nearly zero) at the contact point and reaches its maximum value (< 20 nm) at the position of vanishing visibility. This means that the spatial separation between the two interfered rays is non-significant compared with the spatial coherence lengths of LEDs which are several micrometers [4,8,23]. Therefore, the determined coherence lengths in our study are quite pure TCLs.

5. Conclusion

In this paper, we utilized Newton's rings interference, formed in transmutation, in order to present a simple, stable and accurate method to determine the temporal coherence lengths of light emitting diodes. The visibility of the produced ring fringes has a considerable value at the central fringe while it decreases gradually until vanishing when the two interfered rays get out of coherence as we go far from the center of the fringes. This behavior was utilized and recorded automatically from the experimentally obtained interferogram. The recorded data were

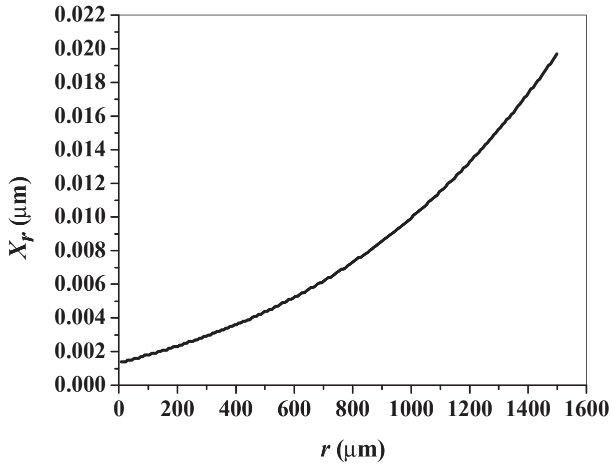

Fig. 7. The relation between the spatial separation distance $X(r)$ between the two interfered rays as a function of the distance measured from the contact point r.

fitted using the logistic function to recognize accurately where the position of minimum visibility locates. The arranged experimental set up was aligned in order to have a single shot image containing the whole formed interference fringes. We applied this method on three light emitting diodes with different wavelengths; 490 nm, 590 nm and 645 nm. The measured temporal coherence length of the three light emitting diodes varied between *ca.* 11 μm and *ca.* 39 μm which are corresponding to temporal coherence time *ca.* 37 fs and *ca.* 130 fs, respectively. The propagating error of the temporal coherence length was determined and the tolerance of the temporal coherence length measurements was less than 5%. Moreover, we proved that the spatial separation distance between the two interfered rays is non-significant compared with the spatial coherence lengths of the used sources. In spite of its simplicity, the presented method is interesting because we were able to measure a quite sensitive temporal coherence length and temporal coherence time. The presented method is very promising where it could be an easy and non-expensive solution to determine the short temporal coherence lengths of organic laser diodes and pulsed lasers.

CRediT authorship contribution statement

W.A. Ramadan: Conceptualization, Methodology, Investigation, Writing - original draft. **H.H. Wahba:** Data curation, Methodology, Software. **A.S. El-Tawargy:** Investigation, Methodology, Visualization, Writing - review & editing.

Declaration of Competing Interest

The authors declare that they have no known competing financial interests or personal relationships that could have appeared to influence the work reported in this paper.

References

[1] C.R. Wheeler, R.D. Ramsier, P.N. Henriksen, An investigation of the temporal coherence length of light, Eur. J. Phys. 24 (2003) 443–450, https://doi.org/10.1088/0143-0807/24/4/363.
[2] S. Yang, A.T. Hammack, M.M. Fogler, L.V. Butov, A.C. Gossard, Coherence length of cold exciton gases in coupled quantum wells, Phys. Rev. Lett. 97 (2006) 187402, https://doi.org/10.1103/PhysRevLett.97.187402.
[3] W.H. Carter, A. Gamliel, E. Wolf, Coherence properties of the field produced by an infinitely large, uniform, planar, secondary Lambertian source, J. Mod. Opt. 41 (1994) 1973–1981, https://doi.org/10.1080/09500349414551861.
[4] G. Xie, M. Chen, M. Mazilu, S. Zhang, A.K. Bansal, K. Dholakia, I.D.W. Samuel, Measuring and structuring the spatial coherence length of organic light-emitting diodes: measuring and structuring the spatial coherence length of organic light-emitting diodes, Laser Photonics Rev. 10 (2016) 82–90, https://doi.org/10.1002/lpor.201500065.
[5] T. Berki, P. Németh, J. Hegedüs, Biological effect of low-power helium-neon (HeNe) laser irradiation, Laser Med Sci. 3 (1988) 35–39, https://doi.org/10.1007/BF02593786.
[6] D. Fixler, H. Duadi, R. Ankri, Z. Zalevsky, Determination of coherence length in biological tissues, Lasers Surg. Med. 43 (2011) 339–343, https://doi.org/10.1002/lsm.21047.
[7] H. Subramanian, P. Pradhan, Y.L. Kim, V. Backman, Penetration depth of low-coherence enhanced backscattered light in subdiffusion regime, Phys. Rev. E 75 (2007) 041914, , https://doi.org/10.1103/PhysRevE.75.041914.
[8] Y. Deng, D. Chu, Coherence properties of different light sources and their effect on the image sharpness and speckle of holographic displays, Sci. Rep. 7 (2017) 5893, https://doi.org/10.1038/s41598-017-06215-x.
[9] H. Lin, P. Yu, Speckle mechanism in holographic optical imaging, Opt. Express 15 (2007) 16322, https://doi.org/10.1364/OE.15.016322.
[10] Z. Cui, A. Wang, Z. Wang, S. Wang, C. Gu, H. Ming, C. Xu, Speckle suppression by controlling the coherence in laser based projection systems, J. Display Technol. 11 (2015) 330–335, https://doi.org/10.1109/JDT.2015.2389233.
[11] J.C. Dainty, A.E. Ennos, M. Françon, J.W. Goodman, T.S. McKechnie, G. Parry, Laser Speckle and Related Phenomena, Springer, Berlin, Heidelberg, 1975.
[12] P.J. de Groot, Applications of optical coherence in interferometric metrology, in: M. Józwik, L.R. Jaroszewicz, M. Kujawińska (Eds.), Speckle 2018: VII International Conference on Speckle Metrology, SPIE, Janów Podlaski, Poland, 2018, p. 48, , https://doi.org/10.1117/12.2319106.
[13] G.O. Reynolds, J.B. DeVelis, G.B. Parrent, B.J. Thompson, The New Physical Optics Notebook, SPIE, 1000 20th Street, Bellingham, WA 98227-0010 USA, 1989. https://doi.org/10.1117/3.2303.
[14] F.J. Duarte, L.S. Liao, K.M. Vaeth, Coherence characteristics of electrically excited tandem organic light-emitting diodes, Opt. Lett. 30 (2005) 3072, https://doi.org/10.1364/OL.30.003072.
[15] D.S. Mehta, K. Saxena, S.K. Dubey, C. Shakher, Coherence characteristics of light-emitting diodes, J. Lumin. 130 (2010) 96–102, https://doi.org/10.1016/j.jlumin.2009.07.027.
[16] F.J. Duarte, Coherent electrically excited organic semiconductors: visibility of interferograms and emission linewidth, Opt. Lett. 32 (2007) 412, https://doi.org/10.1364/OL.32.000412.
[17] S. Reineke, F. Lindner, G. Schwartz, N. Seidler, K. Walzer, B. Lüssem, K. Leo, White organic light-emitting diodes with fluorescent tube efficiency, Nature 459 (2009) 234–238, https://doi.org/10.1038/nature08003.
[18] P.A. Haigh, Z. Ghassemlooy, H. Le Minh, S. Rajbhandari, F. Arca, S.F. Tedde, O. Hayden, I. Papakonstantinou, Exploiting equalization techniques for improving data rates in organic optoelectronic devices for visible light communications, J. Lightwave Technol. 30 (2012) 3081–3088, https://doi.org/10.1109/JLT.2012.2210028.
[19] P.L. Burn, S.-C. Lo, I.D.W. Samuel, The development of light-emitting dendrimers for displays, Adv. Mater. 19 (2007) 1675–1688, https://doi.org/10.1002/adma.200601592.
[20] H.T. Nicolai, A. Hof, P.W.M. Blom, Device physics of white polymer light-emitting diodes, Adv. Funct. Mater. 22 (2012) 2040–2047, https://doi.org/10.1002/adfm.201102699.
[21] J. Blochwitz-Nimoth, O. Langguth, S. Murano, G. He, T. Romainczyk, J. Birnstock, PIN-OLEDs for active-matrix-display use, J. Soc. Inf. Display. 18 (2010) 596, https://doi.org/10.1889/JSID18.8.596.
[22] S.K. Attili, A. Lesar, A. McNeill, M. Camacho-Lopez, H. Moseley, S. Ibbotson, I.D.W. Samuel, J. Ferguson, An open pilot study of ambulatory photodynamic therapy using a wearable low-irradiance organic light-emitting diode light source in the treatment of nonmelanoma skin cancer, Br. J. Dermatol. 161 (2009) 170–173, https://doi.org/10.1111/j.1365-2133.2009.09096.x.
[23] K. Saxena, D.S. Mehta, R. Srivastava, M.N. Kamalasanan, Spatial coherence properties of electroluminescence from Alq3-based organic light emitting diodes, Appl. Phys. Lett. 89 (2006) 061124, , https://doi.org/10.1063/1.2335610.
[24] V. Pourreza Ghoushchi, M. Aas, E. Ulusoy, H. Ürey, Effect of spatial coherence of LED sources on image resolution in holographic displays, in: L.-C. Chien, T.-H. Yoon, S.-D. Lee (Eds.), San Francisco, California, United States, 2017, p. 101260A, , https://doi.org/10.1117/12.2252413.
[25] J. Kim, S. Somani, Y. Yamamoto, Nonclassical Light from Semiconductor Lasers and LEDs, Springer, Berlin, Heidelberg, 2001. http://public.eblib.com/choice/publicfullrecord.aspx?p=3089880 (accessed July 17, 2019).
[26] T. Qureshi, Coherence, Interference and Visibility, Quanta 8 (2019) 24–35 https://doi.org/10.12743/quanta.v8i1.87.
[27] F.J. Duarte, Electrically-pumped organic-semiconductor coherent emission: a review, in: F.J. Duarte (Ed.), Coherence and Ultrashort Pulse Laser Emission, InTech, 2010, , https://doi.org/10.5772/13268.
[28] L.-P. Leppänen, K. Saastamoinen, A.T. Friberg, T. Setälä, Measurement of the degree of temporal coherence of unpolarized light beams, Photon. Res. 5 (2017) 156, https://doi.org/10.1364/PRJ.5.000156.
[29] C.-H. Tsai, K.-C. Tien, M.-C. Chen, K.-M. Chang, M.-S. Lin, H.-C. Cheng, Y.-H. Lin, H.-W. Chang, H.-W. Lin, C.-L. Lin, C.-C. Wu, Characterizing coherence lengths of organic light-emitting devices using Newton's rings apparatus, Org. Electron. 11 (2010) 439–444, https://doi.org/10.1016/j.orgel.2009.11.024.
[30] E. Fazio, G.C. Righini, W.A. Ramadan, M. Bertolotti, Direct measurement of birefringence in ion-exchanged planar waveguides, Opt. Lett. 21 (1996) 1238, https://doi.org/10.1364/OL.21.001238.
[31] M.A. Shams El-Din, W.A. Ramadan, C. Wochnowski, H.H. Wahba, S.S. Aboleneen, Investigation of a UV-laser generated planar polymeric waveguide directly and after

five years of preparation using an interferometric method, Opt. Lasers Eng. 66 (2015) 80–91, https://doi.org/10.1016/j.optlaseng.2014.08.007.
[32] W.A. Ramadan, H.H. Wahba, Lens–fibre interference in measuring liquids' refractive indices, Meas. Sci. Technol. 17 (2006) 215–220, https://doi.org/10.1088/0957-0233/17/1/033.
[33] T.Z.N. Sokkar, M.A. Shams El-Din, A.S. El-Tawargy, On Young's modulus profile across anisotropic nonhomogeneous polymeric fibre using automatic transverse interferometric method, Opt. Lasers Eng. 50 (9) (2012) 1223–1229, https://doi.org/10.1016/j.optlaseng.2012.03.017.
[34] T.Z.N. Sokkar, M.A. Shams El-Din, A.S. El-Tawargy, Effect of recycling on the optical, mechanical and structural properties of polypropylene fibers, Opt. Lasers Eng. 51 (8) (2013) 994–1003, https://doi.org/10.1016/j.optlaseng.2013.02.018.
[35] W.A. Ramadan, H.H. Wahba, M.A. Shams El-Din, Two-dimensional refractive index and stresses profiles of a homogenous bent optical fiber, Appl. Opt. 53 7462 (2014), https://doi.org/10.1364/AO.53.007462.
[36] W.A. Ramadan, H.H. Wahba, M.A. Shams El-Din, Two-dimensional refractive index and birefringence profiles of a graded index bent optical fibre, Opt. Fiber Technol. 36 (2017) 115–124, https://doi.org/10.1016/j.yofte.2017.03.005.
[37] H. Wahba, W. Ramadan, A. El-Tawargy, Optical Fibers Profiling using Interferometric and digital holographic methods, Optical Fiber Applications, IntechOpen, London, UK, 2020, , https://doi.org/10.5772/intechopen.91265.
[38] M.A. Shams El-Din, A.S. El-Tawargy, Interferometric study of the effect of laser intensity and polarization on the cold-drawing of virgin polypropylene fibres, Indian, J. Phys. 91 (2017) 1425–1435, https://doi.org/10.1007/s12648-017-1044-9.
[39] H. Xie, Y. Peng, D. Meng, L. Jiang, Newton's ring and its new discovery, in: Y.C. Chen, D. Fan, C. Gao, S. Zhou (Eds.), Changchun, China, 2006, p. 602825, , https://doi.org/10.1117/12.667338.
[40] D. Malacara (Ed.), Optical shop testing, third ed, Wiley-Interscience, Hoboken, N.J., 2007.
[41] W.A. Ramadan, H.H. Wahba, Simulated Fizeau ring fringes in transmission through spherical and plane reflected surfaces, Appl. Phys. B 124 (2018) 2, https://doi.org/10.1007/s00340-017-6872-y.
[42] W.A. Ramadan, Intensity distribution of Fizeau fringes in transmission with the real path of the interfered multiple-beams, Opt. Lasers Eng. 58 (2014) 27–32, https://doi.org/10.1016/j.optlaseng.2014.01.017.
[43] I.G. Abd El-Sadek, W.A. Ramadan, M. Nawareg, A.S. El-Tawargy, Variable wavelength Newton's rings formed in transmission for measuring radius of curvature and sub-micrometric thin film thickness, Indian, J. Phys. (2019), https://doi.org/10.1007/s12648-019-01570-z.
[44] F.A. Jenkins, H.E. White, Fundamentals of Optics, McGraw-Hill Primis Custom Publ., New York [u.a.], 2010.
[45] F.R. Oliver, Methods of estimating the logistic growth function, Appl. Stat. 13 (1964) 57, https://doi.org/10.2307/2985696.
[46] J.A. Nelder, The fitting of a generalization of the logistic curve, Biometrics. 17 (1961) 89, https://doi.org/10.2307/2527498.